DIFFRACTION OF A SPHERICAL WAVE BY A HARD HALF-PLANE: POLYNOMIAL FORMULATION OF THE EDGE-DIFFRACTED FIELD IN THE FREQUENCY DOMAIN

Djamel Ouis
Department of Architectural Engineering
King Fahd University of Petroleum & Minerals
31261 Dhahran, Saudi Arabia
e-mail: djamel@kfupm.edu.sa

Abstract

The problem of diffraction of a spherical sound wave by a thin hard half-plane is considered. The expression of the total field at any position in the space around the half-plane is composed of two geometrical components and a third one which originating from the edge of the half-plane. This paper takes the expression of the edge-diffracted field due to a sound doublet, as formulated in the Biot-Tolstoy theory of diffraction, BTD, but rearranged for the Dirac-like pulse by Medwin. The present paper presents a development in the frequency domain of the Fourier transform of the exact expression of the edge-diffracted field as given in the time domain. This solution is composed of a serial development, expressed in simple trigonometric integral functions, and which away from the geometrical optics boundaries shows a quite rapid convergence to the numerical Fourier transform of the exact time-domain expression. The presented solution may be used as a good approximation in simulations and in real case predictions of sound scattering by thin straight-edged noise barriers.

Introduction

The problem of sound diffraction by straight edges finds several applications in acoustics, such as in room acoustical studies and simulations (Lau and Tang, 2009; Torres et al, 2001; Vorländer, 2013) or in the development of mathematical models for predicting the sound attenuation in the shadow of noise barriers (Isei et al, 1980; Jonasson, 1972; L'Espérance, 1989; Muradali and Fyfe, 1998; Nicolas et al, 1983; Thomasson, 1978). The scalar acoustical solutions have also been implemented in electromagnetism for the treatment of problems of diffraction of electromagnetic waves by metallic antennas and scatterers. A recent paper by Menounou and Nikolau (2017) reviews some of the theories and models developed through the years for the treatment of diffraction of sound waves by obstacles delimited by sharp straight edges. The problem of diffraction of a spherical wave by a half-plane has been the subject of interest of scientists for an extended period of time. The earliest approach on record was due to Kirchhoff for solving the problem of propagation of a wave through an aperture in a screen with making some reasonable assumptions regarding the value of the field on various regions of the screen (see for instance Bouwkamp, 1954). Sommerfeld's later contribution to the case of scattering by a hard half-plane presented an exact solution for plane wave incidence for either case of perfectly hard or perfectly soft screen (Sommerfeld, 1896). This solution remained under a long time as a reference for comparison with new proposed solutions to similar problems. The concept of multi-valued functions for approaching the solution to the half-plane, and which is elaborated in the frequency domain, inspired several other physical theoreticians to formulating not only more tractable solutions (MacDonald, 1915) but also for treating the case of cylindrical wave incidence (Clemmow, 1950) and even for the more general case of spherical wave incidence (Carslaw, 1899). Several solutions have also been formulated for the more general case of the hard wedge (Carslaw, 1920; MacDonald, 1915), which case is amenable to that of the half-plane. McIver and Rawlins used the method of matched asymptotic expansions for calculating the field in the shadow of a semi-infinite barrier with a finite thickness and having any end impedance on its width (McIver and Rawlins, 1995), or more recently another contribution handling the problem by the method of variables' separation used for solving two-dimensional diffraction problems with bodies having piece-wise linear ideal boundaries (Shanin, 2003).

Another way of approach for handling the problem of sound diffraction by straight edges is through considering the problem in the time domain instead of the frequency domain. An analysis of the problem in the frequency domain would simply be attained through application of the Fourier transform to the expression of the edge-diffracted field as given in the time domain. Hence the solution could be interpreted as the transfer function of the system composed of the pulse source (for generating the sound wave) and the sensing receiver via the space containing the diffracting object. Biot and Tolstoy (1957) proposed in this regard an attractive solution to the case of a perfectly hard wedge problem using the concept of normal coordinates, and which has been revisited during the past four decades. Important applications include the prediction of the sound insulation performance of a hard noise barrier which is simple in shape but can be finite in size (Medwin, 1981), whereas in room acoustics the determination of the impulse response of a closed space in view of hearing simulations, i.e. auralization, may be made more accurate through the inclusion of edge diffraction effects caused by the distribution protuberances on walls or isolated objects within the space under study (Svensson et al., 1999). The classical assumption of the edge-diffracted field as composed of the field generated from the contribution of discrete fictive wave sources located on the edge of the diffracting object becomes therefore more rational. This permits consequently to elaborate powerful and efficient algorithms for simulating the sound field around thick or many-sided screens (Chu et al, 2007). The diverse analytical approaches used for the prediction of the sound field distribution around a noise barrier are usually based on geometrical optics assumptions where the noise barrier is taken as infinite in size. Under reasonable hypotheses on sizes and distances in comparison to the wavelength this permits to consider the expression of the total field at the receiver hidden behind the barrier as composed of the field diffracted at the top edge of the noise barrier. In this respect the noise barrier is mounted on the ground, intercepting the sound path from the noise source to the receiver, and the total field at the observer is considered as made up of four components. The noise source in this context can represent road traffic, and the noise source is in any noise problem in general considered as one of three parts, the two others being the transmission path and the receiver. For a ready-made noise source, tackling a noise problem reduces then to taking measures at the level of the transmission path. In the case of a noise barrier the transmission path is the combination of all lines, single or combined, made by the sound waves in their propagation from the sound source up to the receiver position. For the case of a receiver in the shadow zone behind the barrier, the number of these paths is, to the first order of diffraction, four, and all reach the receiver via the upper edge of the barrier. This is illustrated in Figure 1.

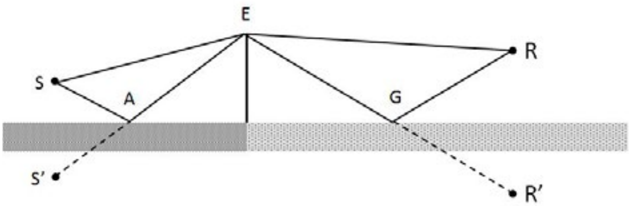

Fig. 1 A noise barrier erected between a sound source and a receiver: The various paths the wave diffracted at the edge of the barrier contributes to the total field at the receiver.

The propagation paths are: S-E-R, S-A-E-R where a reflection of the sound wave on the source side occurs at A, S-E-G-R with a single reflection on the receiver's side at G, and S-A-E-G-R with one reflection on each side of the barrier. All these components of the diffracted field at the top of the barrier are have different amplitudes and phases resulting from different distances to or from the edge of the barrier and different angles of incidence. To that is further included the attenuation and phase shift caused by the sound reflection on the various parts of the ground on either side of the barrier. For applications regarding predictions of road traffic noise attenuation by thin barriers, the problem is amenable to a two-dimensional one with relatively acceptable estimations of the sound field when assuming the traffic line as an extended linear source parallel to the edge of the barrier.

The edge-diffracted field

Considering a point-like sound source emitting a Dirac pulse of strength S, according to the Biot-Tolstoy-Medwin, BTM, theory, the pressure in free space at a distance d from the sound source is given by (Biot and Tolstoy, 1957; Medwin, 1981):

$$u = \frac{\rho S}{4\pi d}\,\delta\left(t - \frac{d}{c}\right) \tag{1}$$

Here ρ is the density of air, c the speed of sound propagation, and δ the Dirac delta function. In presence of a hard half-plane, the edge-diffracted field appears at a time after the source has emitted its pulse, r_0 and r being the normal distances of respectively $\tau_0 = \sqrt{(r + r_0)^2 + z^2}/c$ the source and the receiver to the edge of the half-plane, and z the lateral distance, i.e. the distance along the edge between the projections of both source and receiver positions on the edge of the half plane. The value of is simply the travel time taken by the pulse to reach the receiver via the edge of the half-plane, or the travel time for the shortest possible two-segment distance from sound source to receiver. In the particular case of $z = 0$, the study of diffraction by the half-plane is more simplified as it is amenable to the two-dimensional geometry of Figure 2.

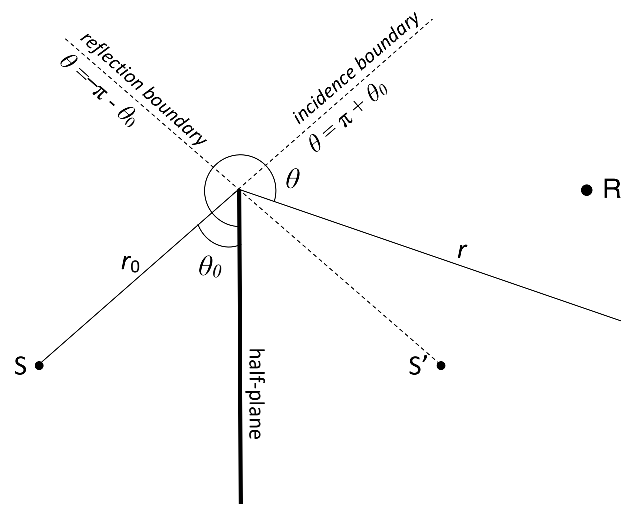

Fig. 2 Two-dimensional geometry of the problem of diffraction of a spherical wave by a half-plane.

When the source and receiver are placed on the same plane normally to the edge of the half-plane, $z = 0$, and the edge-diffracted field takes the expression (Ouis, 2002; and considered again in Appendix A):

$$u_d(t) = \frac{-\rho S}{4\pi^2 c}\sqrt{\frac{{t_+}^2 - {t_-}^2}{t^2 - {t_+}^2}}\left\{\frac{\cos_\pm}{t^2 - {t_+}^2 + \left({t_+}^2 - {t_-}^2\right){\cos_\pm}^2}\right\} \tag{2}$$

For the sake of avoiding unnecessary overload, a full account of the steps that led to this final form is given in detail in Appendix A (see also Ouis, 2002). For writing convenience, here the curly bracket $\{\}_+$ represents the sum of two terms within the bracket and which correspond to the different sign combinations in the argument of the cosine function, i.e. $\cos_\pm = \cos[(\theta \pm \theta_0)/2)]$. Furthermore, $t_\pm = (r \pm r_0)/c$.

The expression of the diffracted field in the frequency domain may be obtained through operating a Fourier transform on the time-domain expression in (2), i.e. (Appendix B).

$$u_d(\omega) = \frac{1}{\sqrt{2\pi}}\int_{-\infty}^{+\infty} u_d(t)e^{i\omega t}dt \sim \int_{t_+}^{+\infty}\frac{1}{\sqrt{t^2 - t_+^2}}\left\{\frac{\cos_\pm}{t^2 - \alpha_\pm}\right\}_+ e^{i\omega t}dt \tag{3}$$

As the diffracted field appears only after traveling the distance from the sound source to receiver via the edge of the half-plane, i.e. it is zero for $t < t_+$, the integration is then to be performed from t_+ to ∞, with the obvious singularity at t_+. An exact analytical expression of the Fourier transform is not available in known tables, and therefore approximations become necessary. Several various forms of such approximations, based mainly on polynomial developments, have been presented in an early paper (Ouis, 2002) and where most of them were based on expressions of the edge diffracted field at times close to t_+ and where most of the sound energy is concentrated. A more recent study has been presented by the author where the expression of the diffracted field has been made through a Fourier analysis of the temporal form of the diffracted field using some special mathematical functions in combination with various polynomial developments (Ouis, 2019). It could be worth mentioning that In this work a new approximation is presented with the expression of the diffracted field being given in terms of a series expansion taking into consideration the expression of the diffracted field at all times following the time of its arrival at the receiver position. It is noted that the denominator of the expression between the brackets in formula (3) can be expressed as $t^2 - \alpha_\pm$ *with* $\alpha_\pm = t_+^2 - 4rr_0 \cos_\pm^2 /c^2 = t_-^2 + 4rr_0 \sin_\pm^2 /c^2 \geq 0$. In this last form the equality $\alpha_\pm = t_+$ is fulfilled only for one of the two components in the expression of the total field and in case the receiver position is at either the geometrical incidence, or reflection boundaries, that is when $\theta = \pi + \theta_0$ *or* $\theta = \pi - \theta_0$ respectively.

In the present work, the integration in (3) is processed through expressing the integrand into an appropriate series expansion. The Fourier transform is then applied to each term of the series expansion resulting in terms containing relatively simply to handle functions involving trigonometric integrals. Hence, and with reference to Eqs. (2-3) the Fourier integration is composed of the sum of 2 terms corresponding to the values of $\alpha_\pm$ according to the signs + and -, as given in Eq. (3) and again reformulated in some more details in (A.5). As the same procedure is taken for both the terms with α_+ and α_- we consider in what fol lows the dummy expression α for meaning either of these two parameters. Hence

$$F(\omega) = \int_{t_+}^{\infty} \frac{e^{i\omega t}}{\sqrt{t^2 - t_+^2}(t^2 - \alpha)} dt \tag{4}$$

or with:

$$K(t) = \frac{1}{\sqrt{t^2 - t_+^2}(t^2 - a)} \tag{5}$$

The integral converges since:

$$\left| \frac{1}{\sqrt{t^2 - t_+^2}(t^2 - a)} e^{i\omega t} \right| \leq K(t) \tag{6}$$

Moreover:

$$I = \int_{t_+}^{\infty} K(t) e^{i\omega t} dt < +\infty \tag{7}$$

Since the value of the integrand is bounded at the limits of the integration sign with an integrable singularity at t_+:

$$K(t) \sim \frac{k_o}{\sqrt{t^2 - t_+^2}} \quad \text{when } t \to t_+ \tag{8}$$

and the decay of the integrand is fast enough to be integrable for large values of the variable, i.e.:

$$K(t) \sim \frac{k_1}{t^3} \quad \text{when } t \to +\infty \tag{9}$$

or some positive k_0 and k_1.

We have for $t > \alpha$ (Spanier and Oldham, 1987, f. 16.6.2, p. 126):

$$\frac{1}{(t^2 - \alpha)} = \frac{1}{t^2} \cdot \frac{1}{1 - \alpha/t^2} = \frac{1}{t^2} \sum_{k=0}^{+\infty} \left(\frac{\alpha}{t^2}\right)^k = \frac{1}{t^2} \sum_{k=0}^{+\infty} \left(\frac{\alpha}{t_+^2}\right)^k \left(\frac{t_+}{t}\right)^{2k} \tag{10}$$

We also have for $t > t_+$ (Spanier and Oldham, 1987, f. 14.6.2, p. 109):

$$\frac{1}{\sqrt{t^2 - t_+^2}} = \frac{1}{t}\left(1 - \frac{t_+^2}{t^2}\right)^{-1/2} = \frac{1}{t} \sum_{j=0}^{+\infty} a_j \left(\frac{t_+}{t}\right)^{2j} \tag{11}$$

with:

$$a_j = \frac{(2j)!}{2^{2j}(j!)^2} \tag{12}$$

Thus:

$$K(t) = \frac{1}{t^3} \sum_{k=0}^{+\infty} b_k \left(\frac{t_+}{t}\right)^{2k} = \frac{1}{t^2} \sum_{k=0}^{+\infty} \frac{b_k}{t_+^3} \left(\frac{t_+}{t}\right)^{2k+3} \tag{13}$$

with:

$$b_k = \sum_{j=0}^{k} a_j \left(\frac{\alpha}{t_+^2}\right)^{k-j} \tag{14}$$

we get then:

$$F(\omega) = \int_{t_+}^{+\infty} K(t)e^{i\omega t}dt = \sum_{k=0}^{+\infty} \frac{b_k}{t_+^3} \int_{t_+}^{+\infty} \left(\frac{t_+}{t}\right)^{2k+3} e^{i\omega t}dt \tag{15}$$

Here the interchange of order between the signs of discrete summation and integration is possible because of the convergence of the integrand, and which is composed of an infinite series of non-negative terms (a consequence of application of the Fubini-Tonelli's theorem, see for instance (Folland, 1999)).

$$F(\omega) = \sum_{k=0}^{+\infty} \frac{b_k}{t_+^2} \int_{1}^{+\infty} \frac{e^{i\omega t_+ s}}{s^{2k+3}} ds \tag{16}$$

Hence with the change of variable $s=t/t_+$. It remains to calculate:

$$I_n(\omega_*) = \int_{1}^{+\infty} \frac{e^{i\omega_* s}}{s^n} ds \tag{17}$$

for $n > 2$. Here $\omega_* = \omega \cdot t_+$

An integration by parts gives:

$$I_n(\omega_*) = -\frac{e^{i\omega_*}}{i\omega_*} + \frac{n}{i\omega_*}\int_{1}^{+\infty} \frac{e^{i\omega_* s}}{s^{n+1}} ds = -\frac{e^{i\omega_*}}{i\omega_*} + \frac{n}{i\omega_*} I_{n+1}(\omega_* \tag{18}$$

Hence:

$$I_{n+1}(\omega_*) = \frac{i\omega_*}{n} I_n(\omega_*) + \frac{e^{i\omega_*}}{n} \tag{19}$$

By induction, it can be shown that we get for n ≥ 2 and for: $\omega_* \neq 0$:

$$I_n(\omega_*) = \frac{(i\omega_*)^{n-1}}{(n-1)!} I_1(\omega_*) + \left(\sum_{k=2}^{n} \frac{(n-k)!}{(n-1)!} (i\omega_*)^{k-2}\right) e^{i\omega_*} \tag{20}$$

with:

$$I_1(\omega_*) = \int_{1}^{+\infty} \frac{e^{i\omega_* s}}{s} ds = \int_{|\omega_*|}^{+\infty} \frac{e^{i\varepsilon t}}{t} dt = -\operatorname{Ci}(|\omega_*|) - i\varepsilon \operatorname{si}(|\omega_*|) \tag{21}$$

in which ε is the sign of ω_* and si and Ci are the sine and cosine integrals respectively (Spanier and Oldham, 1987, f. 38:1:1, p. 361 and f. 38:3:5, p. 365):

$$\operatorname{si}(x) = -\int_{x}^{+\infty} \frac{\sin(t)}{t} dt \quad \text{and} \quad \operatorname{Ci}(x) = -\int_{x}^{+\infty} \frac{\cos(t)}{t} dt\ ; \tag{22}$$

Summing up:

$$F(\omega) = \left(\sum_{k=0}^{+\infty} \frac{b_k}{t_+^2} \frac{(i\omega_*)^{2k+2}}{(2k+2)!}\right) I_1(\omega_*) + \sum_{k=0}^{+\infty} \frac{b_k}{t_+^2} \left(\sum_{m=2}^{2k+3} \frac{(2k+3-m)!}{(2k+2)!} (i\omega_*)^{m-2}\right) e^{i\omega_*} \tag{23}$$

with $\omega_* = \omega \cdot t_+$.

In the plots of Figures 3-5 that follow, a number of only 10 terms were taken in the series expansions given by formula (23). The approximation in these plots is represented by the dashed curve. The continuous line in the plots is the amplitude of the normalized edge diffracted field as calculated by software Wolfram Mathematica, and which is the amplitude in dB of the numerical Fourier transform as given in expression (3). Figure 3 represents a plot for the amplitude of the edge-diffracted field for fixed positions of the sound source and the receiver but for a varying frequency and covering the whole audio range. In contrast, Figures 4 and 5 represent plots of the amplitude of the edge-diffracted field for two different frequencies. In both plots the sound source is kept at a fixed position whereas the receiver position is moving on a circle centered at the edge of the half-plane and covering the whole space surrounding it.

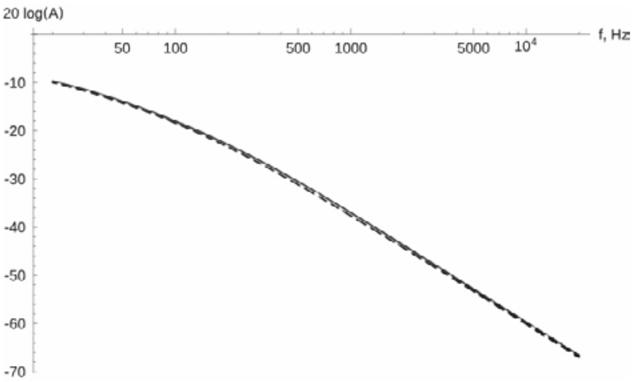

Fig. 3: Relative variation of the amplitude of the edge-diffracted field in dB with frequency in the range [20 Hz - 20.0 kHz]. r_0 = 4.0 m; r = 5.0 m; θ_0 = 30.0o; θ = 240.0º, see Fig. 2 for details. Continuous line: exact numerical Fourier transform; dashed line: approximate, as given in expression (23).

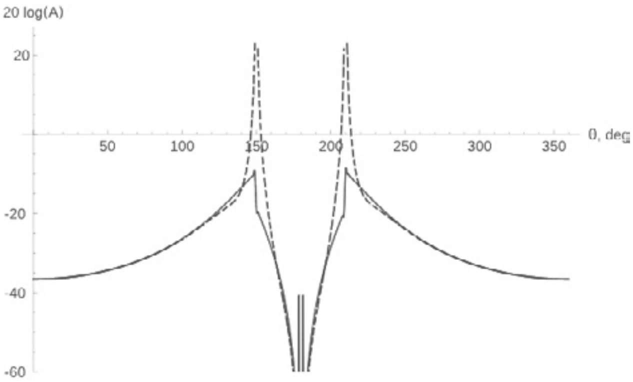

Fig. 4: Variation of the relative amplitude of the edge-diffracted field in dB as function of the receiver angle θ around the half-plane in the range [0.0º - 360.0º]; r_0 = 4.0 m; r = 6.0 m; θ_0 = 30.0º; see Fig. 2 for details. f = 150.0 Hz. Continuous line: exact numerical Fourier transform; dashed line: approximate, as given in expression (23).

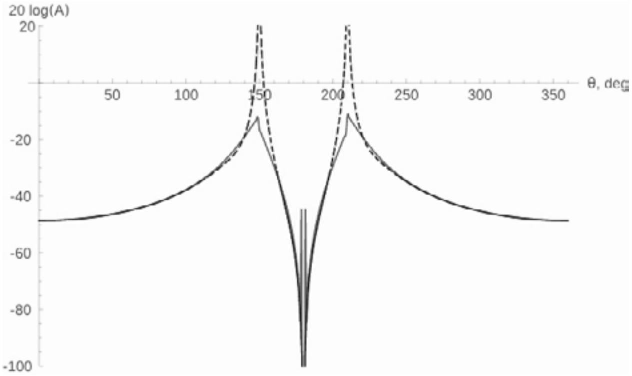

Fig. 5: Relative variation of the amplitude of the edge-diffracted field in dB as function of the receiver angle θ in the range [0.0º - 360.0º]; r0 = 4.0 m; r = 6.0 m; θ_0 = 30.0º; see Fig. 2 for details. f = 500.0 Hz. Continuous line: exact numerical Fourier transform; dashed line: approximate, as given in expression (23).

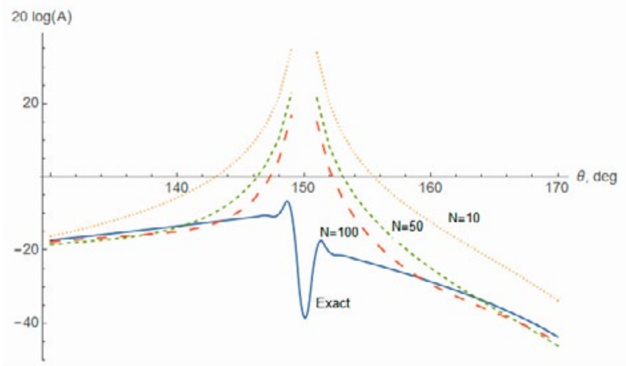

Fig. 6: Relative variation of the amplitude of the edge-diffracted field in dB as function of the number of terms taken in the approximation of expression (23). Details as given in Fig. 4 with expansion of the angle range around the geometrical optics' reflection boundary.

The zones of disagreement between the exact numerical Fourier integration and the approximation shrink considerably when including more and more elements in the series expansions (last term in final form (23)). It would be more objective to analyze the rate of convergence of the series in formula (23), and if defined as $\lim_{k\to\infty} \frac{x_{k+1} - L}{x_k - L}$ where L is the exact value of the expression and x_k the term of order k in the series. However, the difficulty in making a reasonable meaning to such an analysis resides mainly in the consideration of two main facts. First, at the approach to the geometrical reflection and incidence zones, the approximation demarks gradually from the exact value of the diffracted field and the divergence widens considerably the nearer to these zones. The second reason is that the rate of convergence will also depend on the frequency considered in the FT, and the higher the frequency (i.e. the shorter the wavelength as compared to typical distances in the problem) the faster the convergence of the approximation to the exact expression, but then here again the proximity to the geometrical zones plays also an important role.

Regarding the frequency variation of the amplitude of the edge-diffracted field, a relative discrepancy of less than approximately 5% (corresponding to about 0.45 dB) is observed between the exact integration and the proposed approximation for frequencies above a value for which the condition $kR = 5$ is fulfilled, k being the wavenumber and R the longer distance from the edge of the half-plane to either the sound source or the receiver. It may be worthwhile noting the symmetry of the behavior of the amplitude of the edge-diffracted field around the half-plane, and which may be shown as due to exchanging θ by $(2\pi- \theta)$ in Expression (2), and which leads only to a change of sign of the expression following the change of to $cos_{\pm}$ to $-cos_{\mp}$.

Conclusions

In this note the diffraction of a spherical wave by the edge of a hard half—plane was considered. The expression of the edge-diffracted wave in the time domain is exact but does not allow itself for a direct Fourier transform in order to obtain the expression of the edge-diffracted field in closed form in the frequency domain. Hence the time domain expression was reformulated as a combination of terms leading partly to exact integrations and a serial development in view of performing adequate Fourier transforms to the terms in the series expansion. The new approximate expression of the edge diffracted field shows good agreement with that of the numerical integration of the exact time-domain expression in the entire space surrounding the half-plane with an exception at approaching the geometrical reflection and incidence zones. In these zones the field exhibits a singular behavior in an angular region which becomes narrower the higher the frequency. According to the graph of Figure 6 the inclusion of more terms in the approximate series expansion shrinks to some extent the zone of disagreement with the exact numerical integration, but this sets an exponentially increasing load on computation resources. A possible measure to this deficiency in the approximation may be to consider more terms in the series expansion of (B.20) and to consider extrapolating the field between two points on either side of the boundary zones around singularities. This remedy however will depend not only on the frequency considered but also on the geometrical configuration of the problem for the reason that some combination of the source and the receiver positions can lead to violent and erratic variations of the edge diffracted field. An alternative way of treating the problem of diffraction specifically at the reflection and shadow zone boundaries could be through adopting a completely different approach based on considerations of the acoustic energy transported by the edge diffracted pulse. In fact, it can be seen from the time expression of the pressure that this energy is concentrated right after the time of arrival of the diffracted signal. This energy may be considered as the contribution from fictive secondary sources positioned on either side of the point on the edge making shortest the distance from source to receiver via the edge of the half-plane (this point is the apex of the “cone of diffraction” as defined by Keller (1962); the half-plane is a special case of the more general case of the wedge, and where the opening angle extends to 2π). Hence a spatial integration of the expression of the edge-diffracted field centered at this point, and along a definite length on the diffracting edge, gives an accurate value to the early part of the edge impulse response (Svensson and Calamia, 2006). Here the amplitude of the edge diffracted field approaches in magnitude that of the incident field or that of the field at specular reflection at respectively the shadow boundary or the reflection boundary. This is so to ensure a smooth continuity of the total field at transiting through those boundaries, and again the considered frequency will be decisive for the length of the integration path on the edge of the half-plane. For practical applications of usual occurrence, such as calculating the field diffracted around a thin noise barrier, the presented solution gives accurate enough predictions for a barrier with height comparable to or larger than a wavelength.

Appendix A: Development for Equation (2)

For a sound source with strength S in a fluid with density ρ, the incident field u at a receiver point at some distance d from the sound source is:

$$u = \frac{\rho S \delta}{4\pi d}\left(t - \frac{d}{c}\right) \tag{A.1}$$

For a lateral distance $z = 0$ between the sound source and the receiver, the time of arrival of the edge diffracted wave after the source has emitted its pulse is:

$$\tau_0 = (r + r_0)/c \tag{A.2}$$

c being the speed of wave propagation. With reference to Figure 2, and for the general case of a wedge with exterior angle θ_W, the expression for the edge-diffracted field is:

$$u_d(t) = \frac{-S\rho c}{4\pi\theta_W}\{\beta\}\frac{\exp\left(-\nu y\right)}{rr_0 \sinh(y)} \tag{A.3}$$

$\nu = \pi/\theta_W$ being the wedge index, and which takes the value ½ for the half plane.

In (A.3)

$$y = \operatorname{arccosh}\frac{c^2t^2 - (r^2 + {r_0}^2)}{2rr_0} \tag{A.4}$$

and $\{\beta\}$ is in a compact form the sum of 4 fractions resulting from taking the possible combinations of signs in the arguments of the trigonometric functions in:

$$\{\beta\} = \frac{\sin[\nu(\pi \pm \theta \pm \theta_0)]}{1 - 2\exp(-\nu y)\cos[\nu(\pi \pm \theta \pm \theta_0)] + \exp(-2\nu y)} \tag{A.5}$$

For the half plane, the expression for the edge-diffracted field becomes:

$$u_d(t) = \frac{-S\rho c}{8\pi^2}\{\beta\}\frac{1}{rr_0 \sinh(y)}e^{-y/2} \tag{A.6}$$

in which:

$$y = \operatorname{arccosh}(a) = \log\left[a + \sqrt{a^2 - 1}\right] \text{ with } a = \frac{c^2t^2 - (r^2 + r_0^2)}{2rr_0} \tag{A.7}$$

Rewriting (A.5) for the half-plane gives:

$$\{\beta\} = \frac{\sin\left[\frac{(\pi \pm \theta \pm \theta_0)}{2}\right]}{1 - 2e^{-\frac{y}{2}}\cos\left[\frac{(\pi \pm \theta \pm \theta_0)}{2}\right] + e^{-y}} = \frac{\sin[(\pi \pm \theta \pm \theta_0)/2]}{2e^{-y/2}\{\cosh(y/2) - \cos[(\pi \pm \theta \pm \theta_0)/2]\}} \tag{A.8}$$

Next, use is made of the property:

$$\cosh\,(y/2) = \sqrt{(\cosh(y) + 1)/2} \tag{A.9}$$

and of:

$$\sinh y = \frac{e^y - e^{-y}}{2} = \sqrt{\cosh^2 y - 1} = \sqrt{\mathrm{a}^2 - 1} \tag{A.10}$$

The trigonometric expressions in $\{\beta\}$can further be simplified according to the expressions in the table:

	++	+-	-+	—
sin[(π±θ±θ_0)/2]	cos +	cos-	cos-	cos+
cos[(π±θ±θ_0)/2]	-sin+	-sin-	sin-	sin+

(A.11)

with: $$\cos,\sin \pm = \cos,\sin\left(\frac{\theta}{2} \pm \frac{\theta_0}{2}\right) \tag{A.12}$$

Hence:

$$\{\beta\} \sim \frac{1}{2}\left[\frac{\cos +}{x + \sin +} + \frac{\cos -}{x + \sin -} + \frac{\cos -}{x - \sin -} + \frac{\cos +}{x - \sin +}\right] \tag{A.13}$$

where x stands for $x = \cosh\,(y/2) = \sqrt{(\mathrm{a}+1)/2}$. $\{\beta\}$

$\{\beta\}$ then becomes:

$$\{\beta\}\sim x\left[\frac{\cos +}{x^2-\sin +^2}+\frac{\cos -}{x^2-\sin -^2}\right] \quad \text{(A.14)}$$

And u_d takes the form:

$$u_d=\frac{-S\rho c}{8\pi^2}x\left[\frac{\cos +}{x^2-\sin +^2}+\frac{\cos -}{x^2-\sin -^2}\right]\frac{1}{rr_0\sqrt{a^2-1}} \quad \text{(A.15)}$$

Next:

$$rr_0\sqrt{a^2-1}=rr_0\left\{\left[\frac{c^2t^2-(r^2+r_0{}^2)}{2rr_0}\right]^2-1\right\}^{1/2}=\frac{c^2}{2}\sqrt{(t^2-t_+{}^2)(t^2-t_-{}^2)} \quad \text{(A.16)}$$

with:

$$t_\pm=(r\pm r_0)/c \quad \text{(A.17)}$$

Furthermore:

$$rr_0=c^2(t_+{}^2-t_-{}^2)/4 \quad \text{(A.18)}$$

x in (A.13) may also be expressed as:

$$x=\cosh\left(\frac{y}{2}\right)=\sqrt{\frac{(a+1)}{2}}=\frac{c}{2}\sqrt{\frac{(t^2-t_-{}^2)}{rr_0}}=\sqrt{\frac{t^2-t_-{}^2}{t_+{}^2-t_-{}^2}} \quad \text{(A-19)}$$

Then inserting (A.16) and (A.18) into (A.15) gives:

$$u_d=\frac{-S\rho}{8\pi^2c}\sqrt{\frac{t_+{}^2-t_-{}^2}{t^2-t_+{}^2}}\left\{\frac{\cos[(\theta+\theta_0)/2]}{t^2-t_-{}^2-(t_+{}^2-t_-{}^2)\sin^2[(\theta+\theta_0)/2]}+\frac{\cos[(\theta-\theta_0)/2]}{t^2-t_-{}^2-(t_+{}^2-t_-{}^2)\sin^2[(\theta-\theta_0)/2]}\right\} \quad \text{(A.20)}$$

And which gives the expression in Equation (2) after using $\sin^2=1-\cos^2$.

Appendix B: Details for Equation (3)

$$I=\int_{-\infty}^{+\infty}u_d(t)e^{i\omega t}dt \quad \text{(B.1)}$$

with:

$$u_d(t)=\frac{-\rho S}{4\pi^2c}\sqrt{\frac{t_+{}^2-t_-{}^2}{t^2-t_+{}^2}}\left\{\frac{\cos_\pm}{t^2-t_+{}^2+\left(t_+{}^2-t_-{}^2\right)\cos_\pm{}^2}\right\}_+ \quad \text{(B.2)}$$

and $u_d = 0$ *for* $t < t+$. Hence:

$$I=\frac{-\rho S\sqrt{t_+{}^2-t_-{}^2}}{4\pi^2c}\int_{t_+}^{+\infty}\frac{1}{\sqrt{t^2-t_+{}^2}}\left\{\frac{\cos_\pm}{t^2-t_+{}^2+\left(t_+{}^2-t_-{}^2\right)\cos_\pm{}^2}\right\}_+e^{i\omega t}dt \quad \text{(B.3)}$$

with the denominator of the fraction within the bracket in the integrand being expressed as:

$$t^2-t_+{}^2+\left(t_+{}^2-t_-{}^2\right)\cos_\pm{}^2=t^2-t_+{}^2+\frac{4rr_0}{c^2}\cos_\pm{}^2=t^2-\alpha_\pm \quad \text{(B.4)}$$

with:

$$\alpha_\pm=t_+{}^2-\frac{4rr_0}{c^2}\cos_\pm{}^2\le t_+{}^2 \quad \text{(B.5)}$$

References

Biot M.A. and Tolstoy I., 1957, Formulation of wave propagation in infinite media by normal coordinates with an application to diffraction. Journal of the Acoustical Society of America 29, pp 381-391.

Bouwkamp C.J., 1954, Diffraction Theory. Reports on Progress in Physics, 17, pp 35-100.

Carslaw H.S., 1899, Some multi-form solutions of the partial differential equations of physical mathematics and their applications. Proceedings of the Royal Society of London 30, pp 121-161.

Carslaw H.S., 1920, Diffraction of waves by a wedge of any angle. Proceedings of the London Mathematical Society 18, pp 291-306.

Chu D., Stanton T.K. and Pierce A.D., 2007. Higher-order acoustic diffraction by edges of finite thickness Pierce Journal of the Acoustical Society of America 122, pp. 3177-3194.

Clemmow P.C., 1950, A note on the diffraction of a cylindrical wave by a perfectly conducting half-plane. Quarterly Journal of Mechanics and Applied Mathematics 3, pp 377-384.

Folland, G.B., 1999, Real Analysis, Modern Techniques and their Applications, 2nd Edition, Wiley.

Isei T., Embleton T.F.W. and Piercy J.E., 1980, Noise reduction by barriers on finite impedance ground. Journal of the Acoustical Society of America 67, pp. 46-58.

Jonasson H.G., 1972, Sound reduction by barriers on the ground. Journal of Sound and Vibration 22, pp 113-126.

Keller J.B., 1962, The geometrical theory of diffraction, Journal of the Optical Society of America 52, pp 116-130.

Lau S.K. and Tang S.K., 2009, Performance of a noise barrier within an enclosed space. Applied Acoustics 70, pp 50-57.

L'Espérance A. 1989, The insertion loss of finite length barriers on the ground. Journal of the Acoustical Society of America 86 , pp 179-183.

MacDonald H.M., 1915, A class of diffraction problems. Proceedings of the London Mathematical Society 14, pp 410-427.

McIver P. and Rawlins A.D., 1995 Diffraction by a rigid barrier with a soft or perfectly absorbent end face. Wave motion, 22, pp 387-402.

Medwin H., 1981, Shadowing by finite noise barriers. Journal of the Acoustical Society of America 69, pp 1060-1064.

Menounou P. and Nikolaou P., 2017, Analytical model for predicting edge diffraction in the time domain. Journal of the Acoustical Society of America 142, pp 3580-3592.

Muradali A. and Fyfe K.R., 1998, A Study of 2D and 3D Barrier Insertion Loss using Improved Diffraction-based Methods Applied Acoustics 53, pp 49-15.

Nicolas J. , Embleton T.F.W. and Piercy J.E., 1983, Precise model measurement versus theoretical prediction of barrier insertion loss in presence of the ground. Journal of the Acoustical Society of America 73, pp 44-54.

Ouis D., 2002, Diffraction by a hard half-plane: Useful approximations to an exact formulation. Journal of Sound and Vibration 252, pp 191-221.

Ouis D., 2019, Diffraction of a spherical wave by a hard half-plane: Approximation of the edge field in the frequency domain. Journal of the Acoustical Society of America, 145, pp 400-406.

Shanin A.V., 2003, A generalization of the separation of variables method for some 2D diffraction problems. Wave Motion 37, pp 241-256.

Sommerfeld A., 1896¸ Mathematische Theorie der Diffraction, Mathematische Annalen, 37, pp 317-374.

Spanier J. and Oldham K.B., 1987, An Atlas of Functions, Springer Verlag, Berlin.

Svensson U.P. and Calamia P.T., 2006, Edge-diffraction impulse responses near specular-zone and shadow-zone boundaries. Acta Acustica united with Acustica 92, pp 501-512.

Svensson U.P., Fred R.I., Vanderkooy J., 1999, An analytic secondary source model of edge diffraction impulse responses. The Journal of the Acoustical Society of America 106, pp 2331-2344.

Thomasson S.I., 1978, Diffraction by a screen above an impedance boundary. Journal of the Acoustical Society of America 63, pp 1768-1781.

Torres R.R, Svensson U.P. and Kleiner M., 2001, Computation of edge diffraction for more accurate room acoustics auralization. Journal of the Acoustical Society of America 109, pp 600-610.

Vorländer M., 2013, Computer simulations in room acoustics: Concepts and uncertainties. Journal of the Acoustical Society of America 133, pp 1203-1213.

Wolfram Mathematica, 2015, Computing system, Version 10.2.